

# **Optimization for Control of an Integrative System with Thermal and Electrical Storage**

T. Nagai and T. Suzuki

Department of Architecture, Faculty of Engineering, Tokyo University of Science,  
Tokyo 102-0073, Japan

## **ABSTRACT**

The present paper proposes an optimization method for minimizing the electricity consumption or peak electrical demand of a building equipped with both a thermal storage tank and a battery. We use dynamic programming as a dynamic optimization method. In dynamic programming, we need to minimize the number of states and control variables in order to avoid the ‘curse of dimensionality’. Therefore, we use a kW-based approach for modeling components, so that the number of state variables and the number of control variables can be reduced to two each. Based on the proposed optimization method, we investigate optimal scheduling for each objective function such as the cumulative electricity or peak electrical demand, assuming a model office building in Tokyo. For the purpose of minimizing cumulative electricity consumption, the optimization results suggest operations that minimize battery utilization in order to decrease charge and discharge loss. However, for a building equipped with photo-voltaic (PV) panels, there are cases in which it is preferable to use a battery and thermal storage over the weekend, during which the power generated by PV surpasses the electrical load. In order to minimize peak electrical demand, the optimization results indicate the full use of both the battery and thermal storage during peak days. By minimizing the electrical charge, a considerable reduction in peak power is achieved while the cumulative consumption does not increase significantly because the need for the peak reduction is limited to only a couple of days during summer. Finally, we discuss future studies involving the proposed optimization technique.

## **KEYWORDS**

Heat storage, Battery, Optimization, Dynamics, Control

## **INTRODUCTION**

Thermal storage systems are commonly used in heating, ventilating, and air-conditioning (HVAC) systems in order to reduce peak or daytime electrical use. A number of optimal scheduling studies have investigated when to charge heat to or release heat from a thermal storage tank (Braun 1992, Henze et al. 1997, Zhou et al. 2005). Largely as a result of the Tohoku Earthquake in 2011, the use of rechargeable batteries in buildings for supplying electricity, even in the case of a power blackout, has drawn increasing attention in Japan.

However, appropriate operational scheduling remains unclear for the case in which both a thermal storage tank and batteries are installed in the building.

The present paper proposes an optimization method for minimizing the electricity consumption or peak electrical demand of a building equipped with both a thermal storage tank and a battery. We use dynamic programming as a dynamic optimization algorithm. Based on the proposed optimization method, we investigate the optimal scheduling for minimizing each objective function.

## OBJECT SYSTEM

The optimized target is composed of a HVAC system and an electric facility in a building. As shown in Figure 1, the HVAC system includes air handling units, an air-cooled chiller, primary/secondary pumps, and a thermal storage tank. The outdoor conditions and cooling loads of each air-handling unit are all boundary conditions for the optimization. In the present study, we use kW-based modeling for each component. For example, a thermal storage tank is modeled as the following difference equation:

$$q_s(k) = q_s(k-1) - q_{loss}(k) + (q_{in}(k) - q_{out}(k)) \cdot \Delta T \quad (1)$$

where  $q_s$  is the heat quantity stored in the thermal storage tank [kWh],  $q_{loss}$  is the heat loss from the tank during one step [kWh],  $q_{in}$  and  $q_{out}$  are the storing and releasing heating rates [kW], respectively,  $\Delta T$  is the time interval of the optimization calculation, and  $k$  denotes the time step. We use the kW-based approach due to computational efficiency, which is essential for optimization. Under this approach, the heat quantity stored in the tank,  $q_s$ , is the only variable that represents the dynamic state of a HVAC system. In addition, an HVAC system has only one degree of freedom in a time step  $k$ . For example, the cooling power of the chiller [kW] determines all other variables, such as the cooling power,  $q_{out}$ , or the stored heat quantity,  $q_s(k)$ , in the tank, if the value in the previous step,  $q_s(k-1)$ , and the other boundary conditions are given.

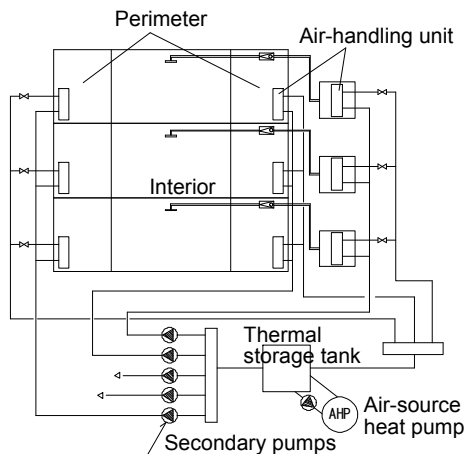


**Figure 1.** HVAC system

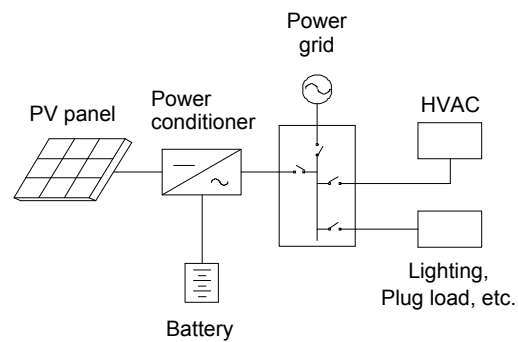


**Figure 2.** Electrical facility inside a building

Figure 2 shows a schematic diagram of the electrical system. The electrical facility in a building is composed of a power receiving facility, a battery, and, in some cases, photovoltaic (PV) panels. The transforming facility distributes electric power to the HVAC system as well as lights, plug loads, etc. The battery and PV panels, if any, are connected to an AC system via a power conditioner (PCS). In the present study, reverse power flow to power grid is not

considered. As is the case of the HVAC system, we use a kW-based approach. The only dynamic state is the electric energy charged in the battery,  $q_b$ . The electric system also has one degree of freedom in one time step  $k$ . For example, the electric charging rate to the battery determines all other variables, such as received electric power or the electric energy charged in the battery,  $q_b(k)$ , if its value in the previous step,  $q_b(k-1)$ , and the other boundary conditions are given.

Altogether, the entire system, i.e., the HVAC and electrical facilities, has two dynamic states and two degrees of freedom.

### OPTIMIZATION METHOD

Mathematical optimization is formulated by an objective function and equality and inequality constraints. In the present paper, the following three objective functions are considered:

- a) Cumulative electric energy received from the power grid,  $E_s$ ,
- b) Peak electrical power received from the power grid,  $E_p$ , and
- c) Electricity cost,  $J_c$ ,

for a certain period, for example, a couple of months. Dynamic programming (DP) (Bellman 1962) optimizes the first two objective functions individually when the target dynamic system is expressed as state transition equations,

$$\mathbf{x}(k) = f(\mathbf{x}(k-1), \mathbf{u}(k), k) \quad \text{for } k = 1, \dots, N \quad (2)$$

under an initial state,  $\mathbf{x}(0) = \mathbf{x}_0$ , where  $\mathbf{x}$  is the state variables vector,  $\mathbf{u}$  is the control variables vector, and  $f$  denotes a function. For the present problem, the vector  $\mathbf{x}$  is two-dimensional, having the heat quantity stored in the tank,  $q_s$ , and the electric energy charged in the battery,  $q_b$ , as components, as described above. The control variables vector,  $\mathbf{u}$ , is also two-dimensional, having the cooling power of the chiller and the electric charging rate to the battery as components. Both the state variables and the control variables are continuous in the present problem and should be discretized over a certain range. Figure 3 shows the backward induction procedure, which is represented as the Bellman equation. Dynamic programming breaks the time-dependent problem into a sequence of time-independent optimization problems.

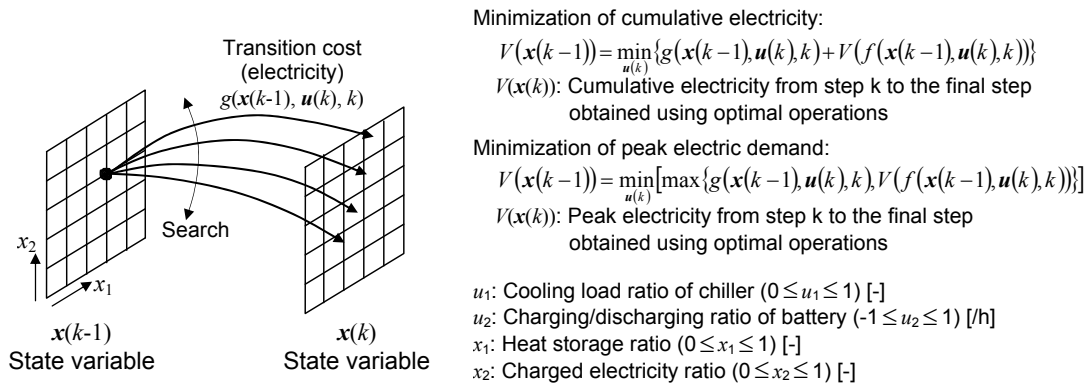


**Figure 3.** Schematic diagram for backward induction in dynamic programming

The last objective function, electricity cost,  $J_c$ , is assumed to be composed of the demand charge and the meter rate and is formulated as follows:

$$J_c = r_p E_p + r_s E_s \quad (3)$$

where  $r_p$  and  $r_s$  are the peak demand charge and the per unit rate, respectively. Here,  $J_c$  is minimized by multi-objective programming, where  $E_p$  and  $E_s$  are objective functions. As shown in Figure 4, the adjoining point of the Pareto solutions curve, and the line expressed by Equation 3 gives the optimal operation that minimizes the objective function,  $J_c$ . Pareto solutions are solutions in which  $E_p$  and  $E_s$  are never improved at the same time by another element of set  $Y$ , where  $Y$  is a set consisting of all combinations  $(E_p, E_s)$  that are derived from all possible control trajectories,  $(\mathbf{u}(1), \mathbf{u}(2), \dots, \mathbf{u}(N))$ , satisfying every constraint considered. Pareto solutions are obtained by DP, minimizing  $E_s$  under various given maximum electric power,  $E_p$ .

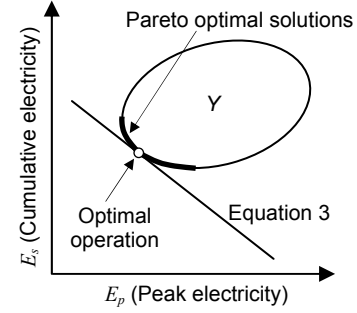


**Figure 4.** Optimization of the weighted sum of two objective functions

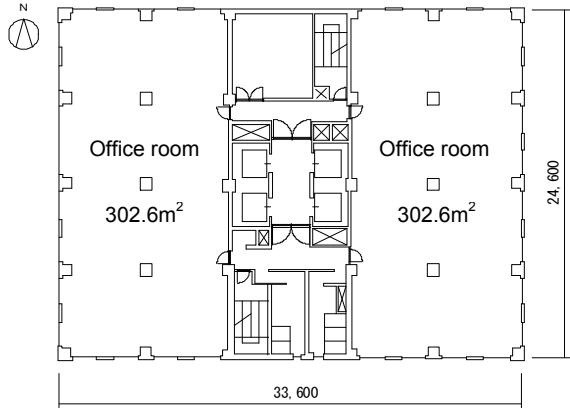
### SIMULATION BLOCK

Here, the simulation block refers to the numerical procedures for calculating the present states,  $\mathbf{x}(k)$ , according to Equation 2. The simulation block also calculates the electric power received from the power grid. In backward induction, which is depicted in Figure 3, the optimization block calls the simulation block and gives  $\mathbf{x}(k-1)$  and  $\mathbf{u}(k)$  for all combinations of these discretized values in each time step. The simulation block calculates the present states,  $\mathbf{x}(k)$ , and the electric power from the power grid and transfers them back to the optimization block. As described above, all of the facility equipment is modeled using a kW-based approach. In the simulation block, a battery is modeled in the same manner as a thermal storage tank, i.e., Equation 1 is also applied to a battery. The component models for a fan, a pump, and a chiller calculate electric consumptions based on their heat load ratios according to the literature (IBEC 1999, MLIT 2011). The PV component merely multiplies the incident solar radiation by its power generation efficiency and outputs the amount as generated power.

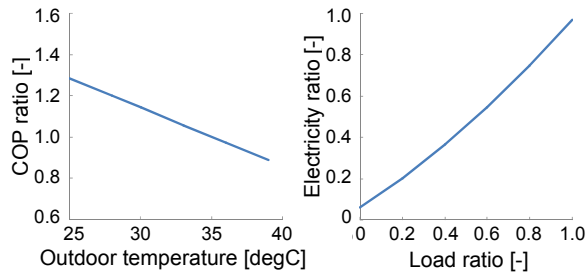
### EXAMPLE BUILDING AND SUBJECT CASES

Figure 5 shows the floor plan of the subject office building, which is a 20-story building in Tokyo, Japan. Tables 1 and 2 show the specifications of the building and the facility, respectively. The office space in each floor is separated into eight zones, each of which is air-conditioned by a dedicated air-handling unit. Prior to optimization, the cooling load of each zone is prepared using the ‘NewHASP/ACLD’ heat load calculation program (JABMEE 2012). Figure 6 shows the performance characteristics of the air-cooled chiller investigated herein. The optimized period is a two months, all of July and August.

Table 3 shows the settings of the subject cases. Case 1 has neither a storage tank nor a battery. In this case, optimization is not carried out, because the degree of freedom of the system is 0, i.e., the operation for each component is determined uniquely. Case 2 has only a storage tank. Cases 3 through 5 have both a storage tank and a battery. The capacity of the storage tank (6,500 kWh) is selected such that the tank supplies a cooling load for 3.5 hours for the design peak load. The chiller capacity is selected among a manufacturer's line-up as low as possible in order to meet the cooling load of the entire building on the cooling design day, assuming that the heat stored in the storage tank is fully released. The battery capacity (600 kWh) is selected such that the battery supplies the daytime electricity load (except that related to HVAC) for approximately one hour. Case 5 has a battery with the double the capacity of that in Cases 3 and 4. Case 4 has PV panels of 160 kW, as well as a storage tank and a battery.



**Figure 5.** Floor plan of the subject office



**Figure 6.** Performance of chiller

## MINIMIZATION OF CUMULATIVE ELECTRICITY

First, we consider the optimization results for the case in which the cumulative electricity received from the power grid is minimized. Figure 7 (left) shows the optimized time evolution for Case 3. The charged electricity ratio<sup>i</sup> remains flat. Since the battery has a charge and discharge loss as well as a self-discharge loss, the battery is not used in order to minimize the cumulative electricity consumption. In contrast, the heat storage ratio<sup>ii</sup> increases at night and decreases during the day. On July 31, the chiller must be operated at night as well as during the day because the daily cooling load is high (17.1MWh), and the chiller capacity is not sufficient if the heat storage is not used. On the next day, the heat storage ratio also increases at night in spite of moderate daily cooling load (10.2MWh). According to Figure 7

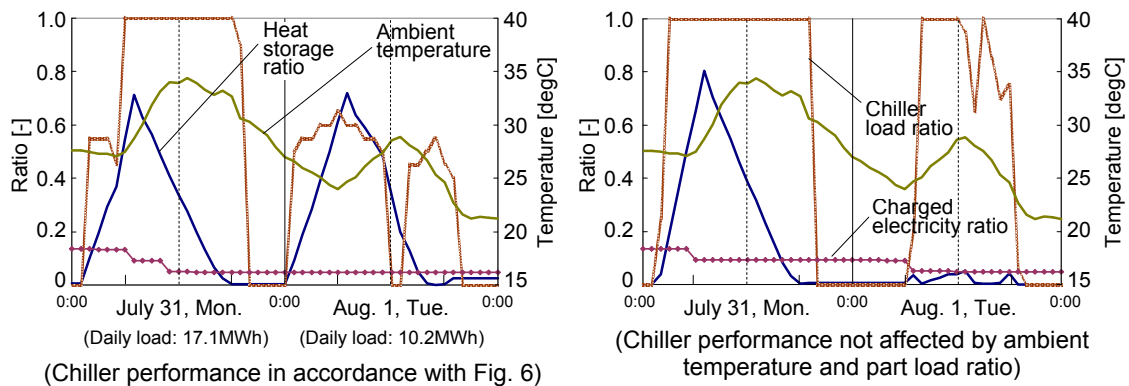


**Figure 7.** Optimal operation for minimizing cumulative electricity consumption (Case3)

**Table 1.** Specifications of the subject building

Usage & site	Office, Tokyo, Japan*
Size	Total area: 16,531m <sup>2</sup> , (20stories)
Occupied hours	8 a.m.-6 p.m.(Weekday)
Temp. setpoint	26degC (Summer), 22degC(Winter)
Internal gains	12 W/(m <sup>2</sup> K) (Lighting), 11 W/(m <sup>2</sup> K) (Plug) (100%) 0.08 person/m <sup>2</sup> (Person)

\*: Expanded AMeDAS Weather Data is used

**Table 2.** Specifications of the subject facility

Chiller	Air-cooled heat pump (1000kW, COP: 3.58)
Control	VAV, VVV(2nd pump), CWV(primary pump)
Heat storage	6,500kWh (Capacity), 5%/day (Heat loss)
Battery	600, 1200kWh (Capacity), 0.85 (Charge+discharge efficiency), 2%/day (Self discharge), 20%/h (Maximum charge/discharge rate)
Power conditioner	0.95 (DC/AC conversion efficiency)
PV panels	160kW (Capacity), 16.0% (Efficiency)
Electricity rates	1,638JPY/kWh (Demand), 13.75YPY/kWh

**Table 3.** Investigated cases

	Chiller* [kW]	Heat storage [kWh]	Battery [kWh]	PV panels [kW]
Case 1	1,700	-	-	-
Case 2	1,000	6,500	-	-
Case 3	1,000	6,500	600	-
Case 4	1,000	6,500	600	160
Case 5	1,000	6,500	1,200	-

\*: Cooling power

<sup>i</sup> The electricity quantity charged in the battery divided by the battery capacity.

<sup>ii</sup> The heat quantity stored in the storage tank divided by the storage capacity.

(right), the heat storage is not used on Aug. 1 if the chiller COP is assumed to be independent of ambient temperature and the part load ratio. Comparison between the two figures implies that it depends on the chiller performance characteristics (Figure 6) as well as daily cooling load and the heat loss from the tank whether the chiller should be operated to store heat at night.

We examine the optimized operation on weekends for Case 4, in which PV panels are installed. When the original settings of the electrical loads are applied, neither the storage tank nor the battery is used. This is because the electricity loads on weekends are larger than the generated PV power. Thus, all generated electricity is consumed directly for electrical demand in the building in order to avoid the charge and discharge loss. Figure 8 shows the optimization results when the electricity loads on weekends are assumed to be 0. If the total charge and discharge efficiency is set to be 0.85, which is the original setting, the generated PV power is used to operate the chiller, and its chilled water is stored in the heat storage tank. In contrast, if the total charge and discharge efficiency is set to be 0.95, the generated power is charged to the battery during the daytime, and the charged electricity is discharged during the night to operate the chiller in order to store chilled water in the storage tank. Operating the chiller at night provides a higher COP because of the lower ambient temperature. Whether the generated PV power is first charged to the battery or is used directly to operate the chiller depends on the magnitude relationship between the total loss associated with the battery and the COP change in ambient temperature.

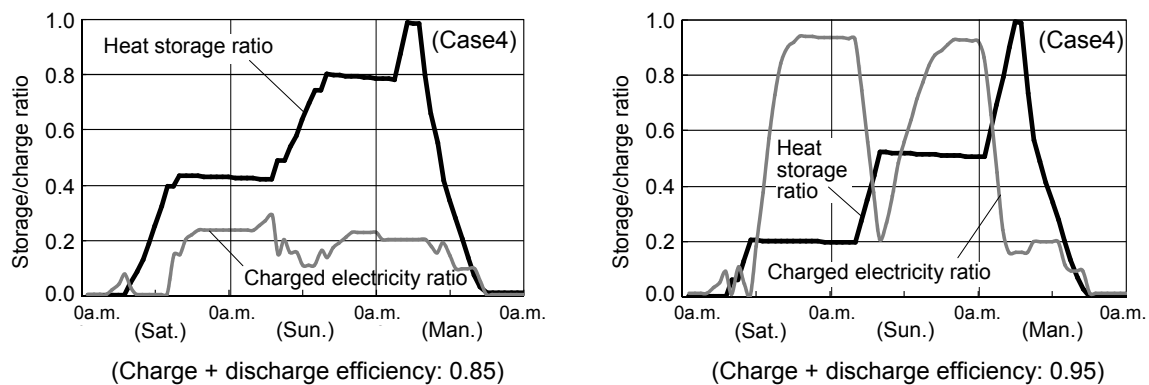


**Figure 8.** Optimal operation on weekends (with PV panels, July 29-31)

### MINIMIZATION OF PEAK ELECTRICAL DEMAND

Next, we examine the optimization results when the maximum electric power received from the grid during the peak hours (from 1 P.M to 4 P.M.) on weekdays is minimized. Figures 9 through 11 show time evolution of the chiller load ratio, the heat storage ratio, the charged electricity ratio, and the electricity power received from the grid on peak summer day (July 31). Figure 9 shows that operating the chiller at full load during the daytime, except during the peak hours, gives the optimal solution regardless of the battery capacity. As shown in Figure 10, the heat storage ratio reaches full capacity before the air-handling units start to operate in the morning. During the daytime, the heat released from the tank is adjusted to the total cooling load, except during the peak hours, when the heat storage ratio decreases so that the total electricity consumption remains flat, as shown in Figure 11. The charged electricity ratio decreases during the peak hours at a maximum rate of 20% of the battery capacity per hour, corresponding to inequality constraint on the battery. This indicates that the maximum admissible discharging rate influences the effect of the battery on the peak reduction. According to Table 4, the thermal storage tank (Case 2) reduces the peak electricity during the peak hours by 32% compared to the reference case (Case 1). In Case 3, in which a battery as

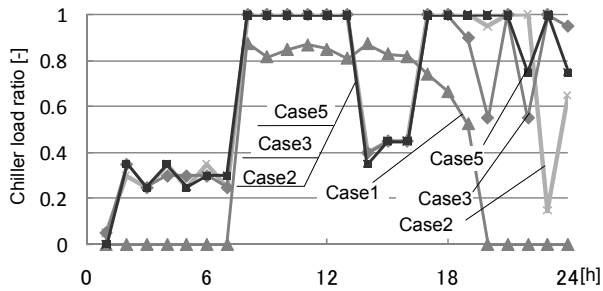


**Figure 9.** Optimal chiller operation for minimizing peak electrical demand

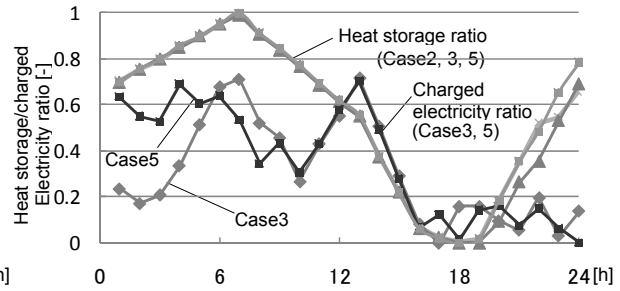


**Figure 10.** Optimized heat storage ratio and charged electricity ratio

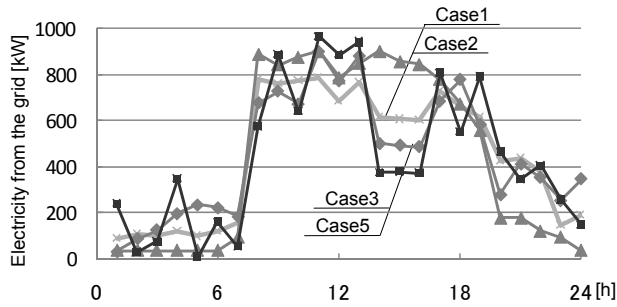


**Figure 11.** Optimized electricity consumption for minimizing peak electrical demand

**Table 4.** Effect of optimization on peak electrical demand

	Peak electricity <sup>*1</sup> [kW]	Peak reduction rate [%]
Case 1	903	-
Case 2	616	32
Case 3	502	44
Case 5	380	58

\*1: from 1 P.M to 4 P.M.

well as a heat storage tank is introduced, the peak electricity decreases by 44% compared to Case 1. In Case 5, in which a battery double the capacity of that for Case 3 is installed, the peak electricity decreases by 58% compared to Case 1.

### MINIMIZATION OF ELECTRICITY COST

Figure 12 shows the Pareto solutions for Case 5. Probably due to discretization, Pareto solutions for extremely low  $E_p$  cannot be obtained. Among the obtained Pareto solutions, the leftmost point gives the optimal operation for minimizing the electricity cost, which is given by Equation 3. As Figure 13 shows, the optimal operation is similar to that for peak minimization (Figures 9-11) on the peak cooling day. In contrast, the optimal operation is similar to that for energy minimization (Figure 7) on off-peak days. According to Figure 12, the curve of the Pareto solutions remains rather flat, i.e., the peak electrical demand during summer is easily reduced without increasing the cumulative electricity. As shown in Figure 14, this is because a limited small number of days are involved in the peak demand during the summer, and the peak-minimization strategy for these days does not noticeably increase the cumulative electricity throughout the entire period.

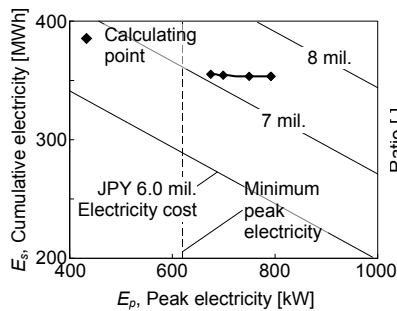


**Figure 12.** Pareto solutions (Case 5, July-Aug.)

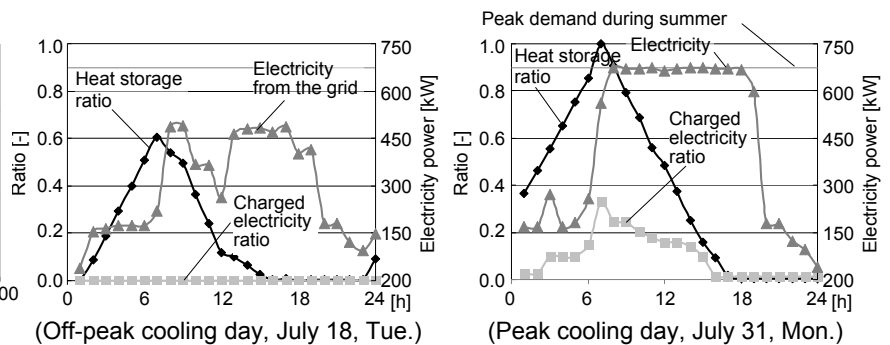


**Figure 13.** Optimized electricity consumption for minimizing electricity cost (Case 5)

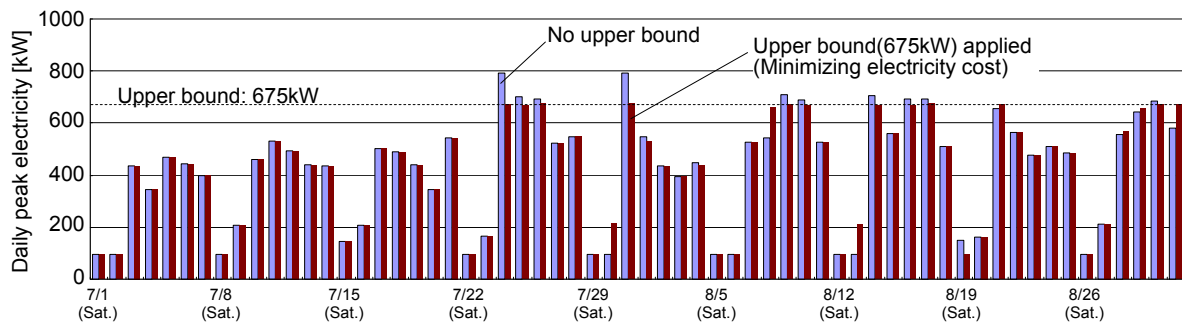


**Figure 14.** Daily peak electrical demand when cumulative electricity is minimized (Case5)

## CONCLUSIONS

The present paper proposed an optimization method to minimize the cumulative electricity, the peak electrical demand, and the electricity cost for the case in which both a heat storage tank and a battery are installed in a building. Dynamic programming and multi-objective programming are used for this purpose. This method suggests an hourly target heat storage ratio and charged electricity ratio. Theoretically, the proposed method is also applicable to cases in which more than one heat storage tank or more than one battery is installed. However, the computational time increases remarkably due to the characteristics of dynamic programming. In the future, it is preferable to consider the uncertainty associated with the next day's load and the model inaccuracy. It is also important to establish a method by which to determine the appropriate target level of peak electrical demand.

## ACKNOWLEDGEMENTS

Special thanks to Katsuhiko Miura, Kuniaki Mihara, and Eikichi Ono, Kajima Technical Research Institute, Tokyo, Japan, for their helpful suggestion to accomplish this paper.

## REFERENCES

- Bellman R. and Dreyfus S. 1962. *Applied dynamic programming*. New Jersey: Princeton University Press.
- Braun J.E. 1992. A Comparison of Chiller-Priority, Storage-Priority and Optimal Control of an Ice-Storage System, *ASHRAE Transactions*. Vol.98, Pt. 1: pp.893-902.
- Henze G.P, Krarti M, and Brandemuehl M.J. 1997. A Simulation Environment for the Analysis of Ice Storage Controls, *HVAC&R Research*. Volume 3, Issue 2 : pp.128-148.
- IBEC. 1999. *BECS/CEC/AC for Windows Operation Manual*. Institute for Building Environment and Energy Conservation. (in Japanese)
- JABMEE. 2012. *New HASP/ACLD Operation Manual*. Japan Building Mechanical and Electrical Engineers Association. (<http://www.jabmee.or.jp/hasp/>, last accessed on 8 July 2012.) (in Japanese)
- MLIT. 2011. *LCEM Tool ver3.03 Calculation Algorithms for Major Objects*. Ministry of Land, Infrastructure, Transport and Tourism. ([http://www.mlit.go.jp/gobuild/sesaku\\_lcem\\_lcem.html](http://www.mlit.go.jp/gobuild/sesaku_lcem_lcem.html), last accessed on 8 July 2012.) (in Japanese)
- Zhou J, Wei G, Turner W.D, Deng S, Claridge D.E, and Contreras O. 1995. Control Optimization for Chilled Water Thermal Storage System Under Complicated Time-of-Use Electricity Rate Schedule, *ASHRAE Transactions*. Vol.111, Pt. 1: pp.184-195.